CLM - P 532

CLM - P 532

UKAEA

Preprint

MEASUREMENT OF THE TEMPORAL EVOLUTION OF THE DISPERSION OF ELECTRON PLASMA WAVES

W H M CLARK

CULHAM LABORATORY
Abingdon Oxfordshire

1978

CLM-P 532

MEASUREMENT OF THE TEMPORAL EVOLUTION OF THE DISPERSION OF ELECTRON PLASMA WAVES

W.H.M. Clark

Culham Laboratory, Abingdon, Oxon, OX14 3DB, UK
(Euratom/UKAEA Fusion Association)

A B S T R A C T

A new technique is described by which the temporal evolution of the wavelength of electron plasma waves in a Q-machine plasma column during a repetitive electron current pulse can be measured.

A consistent analysis of the dispersion curves is presented from which axial velocity moments of up to fourth order of the electron distribution function can be deduced.

(Submitted for publication in Plasma Physics)

April 1978
KS

1. INTRODUCTION

This paper accompanies CLARK and HAMBERGER (1978), hereinafter referred to as I, in that it describes how measurements of the temporal evolution of the dispersion of long wavelength electron plasma waves in a cylindrical, turbulent, plasma column can be used to provide information on the evolution of the electron distribution function of axial velocities, f(v), spatially averaged over scale-lengths of the order of the column radius, a.

Measurements of the dispersion (i.e. frequency $\omega/2\pi$, versus axial reciprocal wavelength $k/2\pi$) of small amplitude waves in a steady-state Q-machine plasma column have been reported in the literature (BARRETT et al 1968, FRANKLIN et al 1974). The results are in very good agreement with the predictions of linear theory where f(v) is assumed to be a Maxwellian. For long wavelengths ($ka \lesssim 1$) the waves are undamped with a dispersion determined in detail by the finite geometry of the plasma column, whereas for short wavelengths ($k\lambda_D \lesssim 1$) Landau damping is observed and the dispersion is unaffected by the finite geometry provided $a >> \lambda_D$.

In I the column is made turbulent by drawing a pulsed electron current of sufficient magnitude for the electron-ion two-stream instability to be excited. Under these conditions fluctuations of density and potential with scale-lengths $\sim \lambda_D$ are expected. Thus the short wavelength dispersion should be drastically affected by the turbulence. However for long wavelengths, most of the electrostatic energy is in the fringing fields which lie outside the plasma. Thus, with a microscopic turbulent scale-length, propagation of such waves

should only be minimally affected by the fluctuations and their dispersion should provide information on f(v) averaged over scale-lengths $\sim$ a. In practice it is found that for a = 1.3 cm, it is not possible to measure wavelengths $\lesssim$ 0.7 cm during the turbulence.

The steady-state measurements are normally made by launching a continuous wave from a small transmitter probe connected to an r.f. oscillator and measuring the axial phase variation using a second, receiving probe connected as an interferometer. In this way the axial wavelength is measured for a given frequency. However the pulsed nature of this experiment (I) makes the usual interferometer technique unsuitable since f(v) and hence the wavelength are changing in time during the pulse. To overcome this problem a sampling technique has been devised which effectively produces "snapshots" of the instantaneous wavelength at a given frequency by recording the instantaneous phase of the received signal as a function of axial position from an ensemble average taken over many pulses. Interpretation of such a measurement is possible if the parameters determining the dispersion are changing on a timescale much longer than the oscillation period, $2\pi/\omega$. In practice this condition is fulfilled for the long wavelength dispersion. Section 2 gives the details of this sampling technique with some typical results. In section 3 a self-consistent analysis of the dispersion curves is presented from which the temporal evolution of the low order velocity moments of f(v) can be deduced.

2. EXPERIMENTAL TECHNIQUE

Figure 1 shows the layout of the experiment. As detailed in I, pulsed electron currents are drawn through the plasma by applying positive voltage pulses (repetition rate 100 - 1000 s^{-1}, duration 2 μs) to the cold plate of the Q-machine from the main pulse generator.

Figure 2 shows the design of the axially movable probes which launch and detect the waves in the plasma column (radius a = 1.3 cm) which is concentric with a cylindrical copper waveguide (radius b = 2.6 cm). As will become clear in section 3, an accurate measurement of the steady-state dispersion is necessary to interpret the dispersion during the pulse. Hence the design of the probes. The loop part of each probe preferentially couples to the lowest order (0,0) eigenmode for long wavelengths ($ka \lesssim 1$) but does not couple to the short wavelength ($ka \gg 1$) modes for which the cross-wire is effective. The waveguide has a cut-off frequency $\simeq 5$ GHz, so that electromagnetic resonances and direct electromagnetic coupling between the probes are considerably diminished for frequencies of interest, (< 1 GHz). This configuration helps to give clean interferometer traces. Also the 250 MHz filter is necessary to cut out the low frequency fluctuations associated with the turbulence.

The transmitter probe continuously excites an electron plasma wave at a fixed frequency, $\omega/2\pi$, (typically 300 - 800 MHz). The sampling unit is set to the "manual" mode so that it samples the amplitude of the received signal, while the sampling gate is open (duration 360 ps $\ll \frac{1}{\omega}$), at a fixed time delay t_o, from the start of each current pulse. The d.c. output of the sampling unit is the amplitude of the sample at $t = t_o$, averaged over many pulses by the external integrating circuit. As the transmitter-receiver separation z, is slowly increased (at a rate ~ 2 mm s^{-1}), the d.c. output varies sinusoidally with the instantaneous phase of the wave as it changes along the column, providing the phase of the transmitted signal does not change from sample to sample. This condition is maintained by triggering the sampling unit with a signal derived from both the voltage pulse and

the transmitted signal as shown in Fig. 3. With this arrangement the sampling gate opens at a fixed phase of the transmitted signal and at a fixed time delay t_o, but with a small jitter on the latter $\ll 2\pi/\omega$. Thus the received signal is,

$$R(t) = A\cos\,[k(t)z - \omega t] \qquad \ldots\ (1)$$

where

$$\left| \frac{1}{k} \frac{dk}{dt} \right| \ll \omega \qquad \ldots\ (2)$$

The sampling unit measures the signal at $t = t_o$ so that the d.c. output is,

$$Y(z) = \langle A\cos[k(t_o)z - \omega t_o]\rangle$$

$$= A\cos[k(t_o)z - \delta] \qquad \ldots\ (3)$$

where $\delta = \omega t_o$ is a constant phase angle. $Y(z)$ is plotted on an X-Y pen recorder from which $2\pi/k(t_o)$ can be measured. Measurement of wavelengths parallel and antiparallel to the electron current are made by interchanging transmitter and receiver although the receiver will detect both waves, particularly at very long wavelengths, because of reflections at the column end plates. In practice, for moderate wavelengths, this is not a serious problem because the reflected signals are very weak.

For very long wavelengths the interferometer trace will have a beat pattern as shown in Fig. 4(i). The two wavelengths can be separated by allowing the time delay for the sampling gate to vary in proportion to the transmitter-receiver separation. This is achieved by applying the voltage from the axial position-sensing potentiometer to the "external sweep" input of the sampling unit and using the unit in the "external sweep" mode. The time delay per unit distance α, is adjusted using the "external sweep attenuator" control, so that there is no phase variation with distance for one of the waves, but the phase variation of the other

wave is increased. The received signal is effectively sampled in the inertial frame of the wave with stationary phase and the observed frequency of the other is doppler-shifted from the laboratory frame.

Thus the received signal for very long wavelengths is:

$$R(t) = A\cos[k_+(t)z - \omega t] + B\cos[k_-(t)z + \omega t] \quad \ldots\ (4)$$

where $2\pi/k_+$ and $2\pi/k_-$ are the wavelengths of waves propogating in the $+z$ and $-z$ directions respectively and $k_+ \approx k_-$. The sampling unit measures the signal at $t = t_o + \alpha z$ where

$$\omega^{-1} < \alpha z_{max} << \left| \frac{1}{k_\pm} \frac{dk^\pm}{dt} \right|^{-1}. \quad \ldots\ (5)$$

Condition (5) requires that the maximum time-delay change αz_{max}, is much shorter than the time-scale for change in wavelength. (In practice $_{max} \leq 30$ cm). Thus the d.c. output to the X-Y pen recorder is,

$$Y(z) = \langle A\cos[k_+(t_o)z - \omega t_o - \alpha\omega z] + B\cos[k_-(t_o)z + \omega t_o + \alpha\omega z]\rangle. \quad \ldots\ (6)$$

If α is adjusted such that,

$$k_+(t_o) = \alpha\omega \quad \ldots\ (7)$$

then (6) becomes,

$$Y(z) = A\cos\delta + B\cos[k_{eff}.z + \delta]. \quad \ldots\ (8)$$

The effective wavelength $2\pi/k_{eff}$ is related to the wavelength in the laboratory frame by,

$$k_- = k_{eff} - \alpha\omega. \quad \ldots\ (9)$$

Notice that k_+ may be computed from (7), but in practice better accuracy is achieved if the process is repeated with $k_- = -\alpha\omega$. A worked example is shown in Fig. 4.

Figure 5 shows typical moderate wavelength interferometer traces

taken at different times for a particular transmitter frequency. At the start of the current pulse ($t = 0$), the parallel and antiparallel wavelengths are equal. During the interval $0 < t < 0.2$ μs, the parallel wavelength is axially non-uniform whereas the antiparallel wave disappears if ω is close to the electron plasma frequency ω_{pe}. After this initial period the antiparallel wave reappears and both wavelengths are axially uniform, tending to increase with time. This behaviour is generally observed under conditions where the plasma is unstable (see I), the time taken for axial uniformity to be established tending to be longer for smaller electron currents. When the plasma is stable the technique is insensitive to the small changes in wavelength that occur.

It is possible to plot the wave dispersion curve at different times during the pulse when the wavelengths are axially uniform. Fig. 6 shows a typical example where the solid lines are fitted theoretical curves using the analytical procedure described in the next section. It can be seen that, after the short time interval of 0.2 μs, an axially uniform electron drift exists in the column causing the dispersion curve to be doppler-shifted from its value at $t = 0$. The non-uniform nature of the parallel wavelength in Fig. 5 indicates that the establishment of the electron drift occurs during the initial transient as it propagates along the column from the cold plate. Further discussion of this transient is given in I.

3. ANALYSIS OF THE DISPERSION CURVES

In contrast to the usual theoretical problem, we wish to evaluate the electron distribution function $f(v)$, from the dispersion of electron plasma waves. Although $f(v)$ can be determined in principle from a complete knowledge of the wave dispersion, a limited number of

experimental points provides restricted information of f(v), i.e. the fitting parameters are in terms of the low order velocity moments of f(v). The following analytical procedure is systematic in that the velocity moments are fitted in sequence with decreasing precision, starting with the zero order (density), followed by the first order (drift velocity) etc up to the fourth order, beyond which the uncertainty in the estimate exceeds the estimate itself.

In the appendix it is shown that the dispersion relation for the (0,0) eigenmode of the column may be written as,

$$\frac{\omega^2}{\omega_{pe}^2} = G(k) \int_{-\infty}^{+\infty} \frac{n^{-1} f(v)dv}{\left(1 - \frac{kv}{\omega}\right)^2} \qquad \ldots\ (10)$$

where G(k) is a function which depends on the radial plasma density profile and the radial boundary conditions. In the experiment the change in dispersion from the initial form at t = 0 is measured, so that if we assume the density profile does not alter between 0 and t, G(k) can be eliminated by taking the ratio of two frequencies for a given value of k, i.e.

$$\left(\frac{\omega_t}{\omega_o}\right)^2 = \frac{\int \frac{f(v)dv}{(1 - kv/\omega)^2}\Big|_t}{\int \frac{f(v)dv}{(1 - kv/\omega)^2}\Big|_{t=0}} \qquad \ldots\ (11)$$

where wave k has frequencies ω_t at time t and ω_o at t = 0. If ω/k has a small imaginary part, then the integrals can be evaluated to a good approximation by assuming ω/k as real and taking the principal value, (JACKSON, 1960). For $(\omega/k)^2 > v^2$, the denominator can be expressed as a binominal expansion and if we further assume that f(v) = 0 for $v^2 \geq (\omega/k)^2$ then,

$$\int_{-\infty}^{+\infty} \frac{f(v)dv}{\left(1 - \frac{kv}{\omega}\right)^2} \simeq \int_{-\infty}^{+\infty} f(v) \left[1 + \frac{2kv}{\omega} + 3\left(\frac{kv}{\omega}\right)^2 + \ldots\right]dv$$

$$= \sum_{p=0}^{\infty} (p + 1) \frac{A_p}{(\omega/k)^p} \qquad \ldots\ (12)$$

where

$$A_p \simeq \int_{-\infty}^{+\infty} v^p f(v)dv \qquad \ldots\ (13)$$

$$A_o = n. \qquad \ldots\ (14)$$

If we assume that the dispersion at t = 0 is that of a cold plasma, the integral in the denominator of (11) is equal to n_o. Thus (11) becomes:

$$\left(\frac{\omega_+}{\omega_o}\right)^2 = \frac{1}{n_o}\left[A_o + \frac{2A_1}{|\omega/k|} + \frac{3A_2}{|\omega/k|^2} + \ldots\right]$$

$$\left(\frac{\omega_-}{\omega_o}\right)^2 = \frac{1}{n_o}\left[A_o - \frac{2A_1}{|\omega/k|} + \frac{3A_2}{|\omega/k|^2} - \ldots\right]. \qquad \ldots\ (15)$$

Where the + and - subscripts refer to parallel and antiparallel propagation respectively. Adding and subtracting the expansions (15) for frequency ratios which have the same phase speed $|\omega/k|$, leads to:

$$\tfrac{1}{2}\Sigma = \tfrac{1}{2}\left\{\left(\frac{\omega_+}{\omega_o}\right)^2 + \left(\frac{\omega_-}{\omega_o}\right)^2\right\} = \frac{1}{n_o}\left[A_o + 3A_2\zeta + 5A_4\zeta^2 \ldots\right]$$

$$\frac{\frac{1}{2}}{\sqrt{\zeta}}\Delta = \frac{1}{2\sqrt{\zeta}}\left\{\left(\frac{\omega_+}{\omega_o}\right)^2 - \left(\frac{\omega_-}{\omega_o}\right)^2\right\} = \frac{1}{n_o}\left[2A_1 + 4A_3\zeta \ldots\right] \qquad \ldots\ (16)$$

where

$$\zeta = \frac{1}{(\omega/k)^2}. \qquad \ldots\ (17)$$

Thus Σ and $\Delta/\sqrt{\zeta}$ can be computed from the dispersion data taken at time t, and t = 0, and plotted as a function of ζ. Even and odd moments of f(v) can be deduced from the coefficients of a least squares polynominal fit, (in practice no higher than a quadratic), to the two

plots, an example of which is shown in Fig. 7.

The three assumptions that lead to the expansions (16) can be checked a posteriori. Firstly the assumption that the radial density profile, which affects the long wavelength ($ka < 1$) dispersion, does not change between 0 and t: inspection of the plots of Σ and $\Delta/\sqrt{\zeta}$ for small ζ in Fig. 7 indicates that this is not the case. After the coefficients A_p have been fitted to the plots, neglecting the points at small ζ, it is possible to work backwards from the small ζ data and determine how the G(k) function has changed between 0 and t due to a change in the radial profile. Fig. 8 shows an example of the corresponding change of the long wavelength dispersion, as viewed from the electron drift frame, suggesting that the density profile broadens during the pulse, although it is difficult to deduce quantitative data from such a measurement; (for an illustration of the dependence of the dispersion on the radial density profile see Barret et al).

Secondly the assumptions concerning the validity of expansion (12) can be checked by ensuring that velocities computed from the fitted coefficients are much smaller than the phase velocities of the waves used in the analysis. A consequence of this is that the value of $\frac{1}{2}\Sigma$ must always be close to unity, (in practice $0.8 < \frac{1}{2}\Sigma < 1.4$).

Thirdly, the assumption that the dispersion for a cold plasma can be used at $t = 0$ is checked by estimating the correction to (15) for a finite temperature at $t = 0$; i.e. if

$$\left(\frac{\omega_o}{\omega_{pe}}\right)^2 \simeq G(k)\left[1 + \frac{3v_{eo}^{\,2}}{(\omega_o/k)^2}\right] \qquad \ldots\ (18)$$

where $v_{eo} = 2 \times 10^7$ cm s^{-1} (corresponding to a temperature of 2,500 K), then the correction to term A_2 in expansion (16) is $\sim v_{eo}^{\,2}$ and the correction to term A_3 is $\sim 3/2\ v_{eo}^{\,2}\ v_d$ etc. These corrections are

smaller than the uncertainties in the estimates of A_2 and A_3.

In order to achieve a reasonable accuracy with the analysis, about forty points are required for each dispersion curve so that collecting the data is time consuming. A simple modification to the basic technique which speeds the process up is to sweep the transmitter frequency with a constant transmitter-receiver separation (CLARK, 1976). Figure 9 shows an example of the analysis where the evolution of the first five velocity moments in the electron rest frame is plotted against t, where,

$$
\begin{aligned}
v_d &= \frac{1}{n}\int_{-\infty}^{+\infty} vf(v)dv \\
v_e^{\,2} &= \frac{1}{n}\int_{-\infty}^{+\infty} (v-v_d)^2 f(v)dv \\
v_a^{\,3} &= \frac{1}{n}\int_{-\infty}^{+\infty} (v-v_d)^3 f(v)dv \\
v_b^{\,4} &= \frac{1}{n}\int_{-\infty}^{+\infty} (v-v_d)^4 f(v)dv.
\end{aligned}
\qquad \ldots\ (19)
$$

This data was taken under conditions where electron heating is expected (see I) and illustrates two properties of the technique. Firstly the measurements are sensitive to velocity changes $\gtrsim v_{eo}$, the initial thermal velocity. Secondly the uncertainty in the estimate of each moment increases with the order of the moment; typical uncertainties are, density 1 - 5%, drift velocity 5 - 10%, thermal velocity 10 - 20% etc. A discussion on the implication of these results is given in I.

4. SUMMARY

In conclusion, a technique has been described which allows the temporal evolution of the dispersion of electron plasma waves to be measured in a turbulent plasma column for wavelengths $\gtrsim$ a. This

technique has been applied to a plasma during a pulsed electron current and the changes in the dispersion have been used to study the evolution of low order velocity moments of the distribution of electron axial velocities averaged over a scale-length $\sim a$.

ACKNOWLEDGEMENT

The author is pleased to acknowledge useful discussions with Dr R.N. Franklin and Dr S.M. Hamberger.

During the period of this work the author was a member of the Department of Engineering Science, Oxford University on attachment to Culham Laboratory.

APPENDIX

Following the analysis given by Franklin et al the eigenmode solutions for the plasma column take the form,

$$\phi(r,\theta,z,t) = R_\mu(r)\ e^{i\mu\theta}\ e^{i(kz - \omega t)} \qquad \ldots\ (A1)$$

where the electrostatic potential ϕ, is a solution of

$$\underline{\nabla}.(\underline{\underline{\varepsilon}}\ \underline{\nabla}\ \phi) = 0. \qquad \ldots\ (A2)$$

In the frequency region,

$$\omega^2_{ce} >> \omega^2_{pe} \gtrsim \omega^2 >> \omega^2_{pi} \qquad \ldots\ (A3)$$

the plasma dielectric tensor is well approximated by

$$\underline{\underline{\varepsilon}} = \begin{pmatrix} 1,0,0 \\ 0,1,0 \\ 0,0,\varepsilon_3 \end{pmatrix} \qquad \ldots\ (A4)$$

where

$$\varepsilon_3(\omega,k,r) = 1 - \frac{e^2}{\varepsilon_o m}\ \frac{\rho(r)}{k^2}\ \int_{-\infty}^{+\infty} \frac{\frac{\partial F(v)}{\partial v}\ .\ dv}{(v - \omega/k)} \qquad \ldots\ (A5)$$

$\rho(r)$ is the radial electron density profile and $F(v)$ is the normalised velocity distribution function which is assumed to be spatially homogeneous.

Substitution of (A1), (A4) and (A5) into (A2) yields the differential equation for R_μ

$$r^2 \frac{d^2R_\mu}{dr^2} + r \frac{dR_\mu}{dr} - \{[1 + \rho(r)\ h(\omega,k)]\ k^2r^2 + \mu^2\}R_\mu = 0 \qquad \ldots\ (A6)$$

where

$$h(\omega,k) = -\frac{e^2}{\varepsilon_o m} \int_{-\infty}^{+\infty} \frac{\frac{\partial F}{\partial v}\ .\ dv}{(v - \omega/k)}. \qquad \ldots\ (A7)$$

At the waveguide wall the potential must vanish, hence the boundary condition,

$$\phi(r = b) = 0 \qquad \ldots\ (A8)$$

determines the dispersion relation for a prescribed $\rho(r)$ because by integrating (A6) with prescribed values of k and μ from r = 0 tor = b, the values of h which make R vanish at r = b can in principle be determined; i.e. for the prescribed variable k, the boundary condition (A8) determines an eigenvalue equation

$$h = g_{\mu\nu}(k) \qquad \ldots\ (A9)$$

for a prescribed function $\rho(r)$ such that equation (A7) can be solved for ω, i.e.

$$g_{\mu\nu}(k) = -\frac{e^2}{\varepsilon_o m k^2} \int_{-\infty}^{+\infty} \frac{\frac{\partial F}{\partial v} \cdot dv}{(v - \omega/k)} \qquad \ldots\ (A10)$$

μ and ν are the azimuthal and radial mode numbers respectively. Integrating (A10) by parts and defining some suitable mean density n, we obtain the form of the dispersion relation for the lowest order ($\mu = \nu = 0$) mode used in section 3, viz;

$$\frac{\omega^2}{\omega_{pe}^2} = G(k) \int_{-\infty}^{+\infty} \frac{n^{-1} f(v) dv}{\left(1 - \frac{kv}{\omega}\right)^2} \qquad \ldots\ (A11)$$

where $$G(k) = \frac{1}{n g_{oo}(k)} \cdot$$

REFERENCES

BARRET, P.J., JONES, H.G. and FRANKLIN, R.N. (1968) Plasma Physics 10, 911.

CLARK, W.H.M. (1976) D.Phil. Thesis, Oxford University (unpublished).

CLARK, W.H.M. and HAMBERGER, S.M. (1978) Plasma Physics, accompanying paper. (CLM-P 532).

FRANKLIN, R.N., HAMBERGER, S.M., LAMPIS, G and SMITH, G.J., (1974) UKAEA, Culham Laboratory Report, CLM-R131, HMSO.

JACKSON, J.D. (1960) J. Nucl. Energy. Part C: Plasma Physics 1, 171.

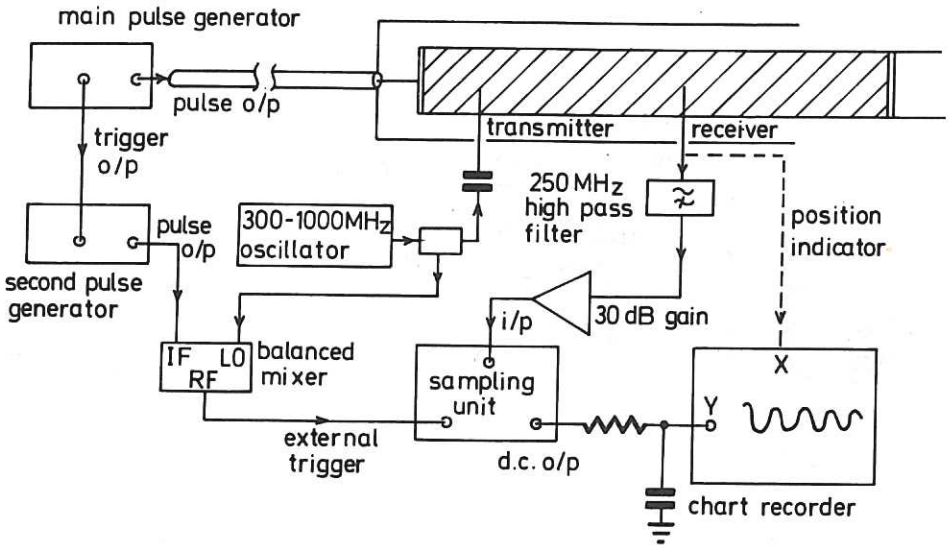

Fig.1 Electronic circuit for the experiment.

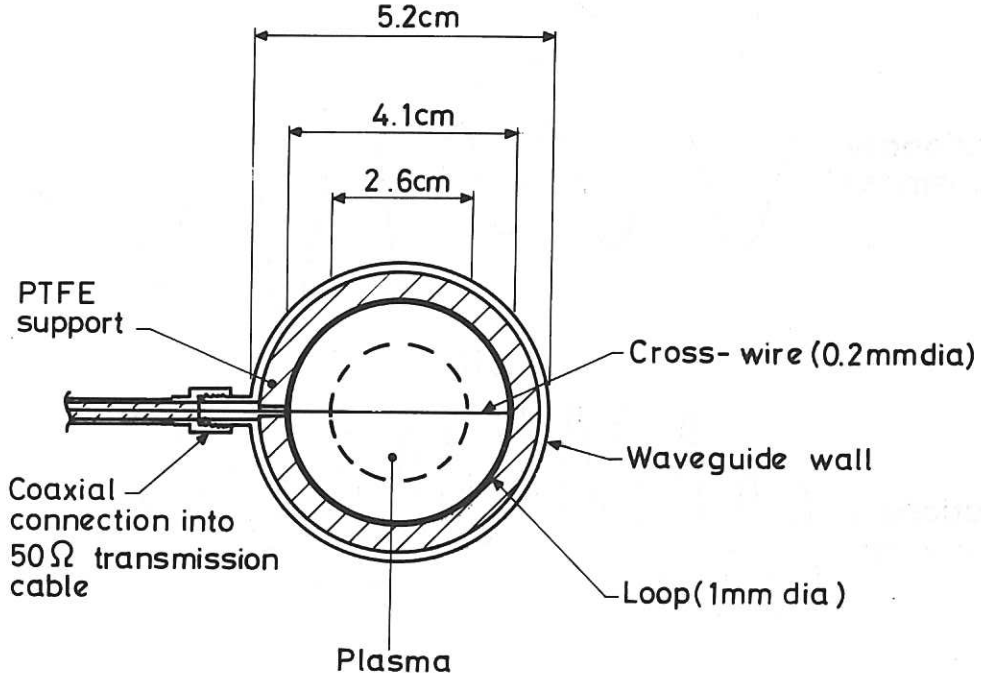

Fig.2 Design of transmitter/receiver probes.

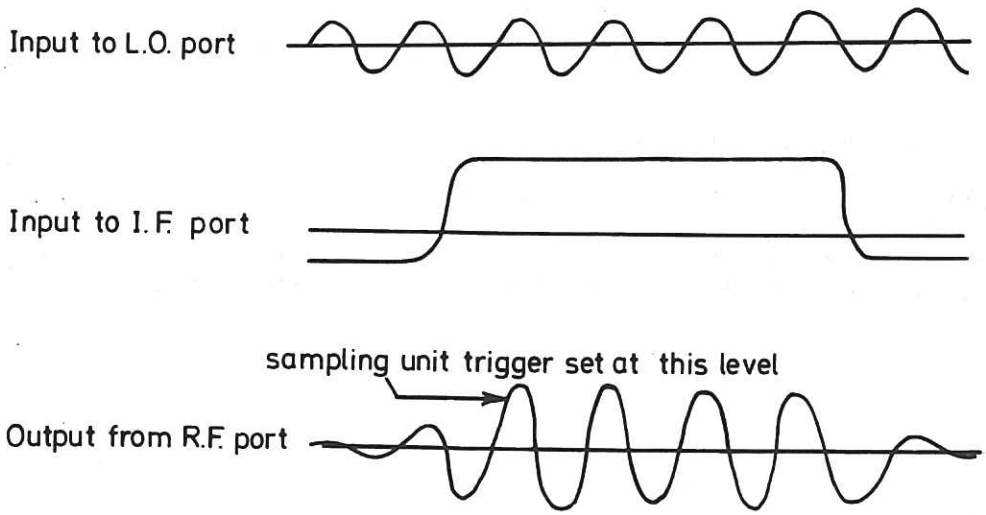

Fig.3 Input and output signals to balanced mixer.

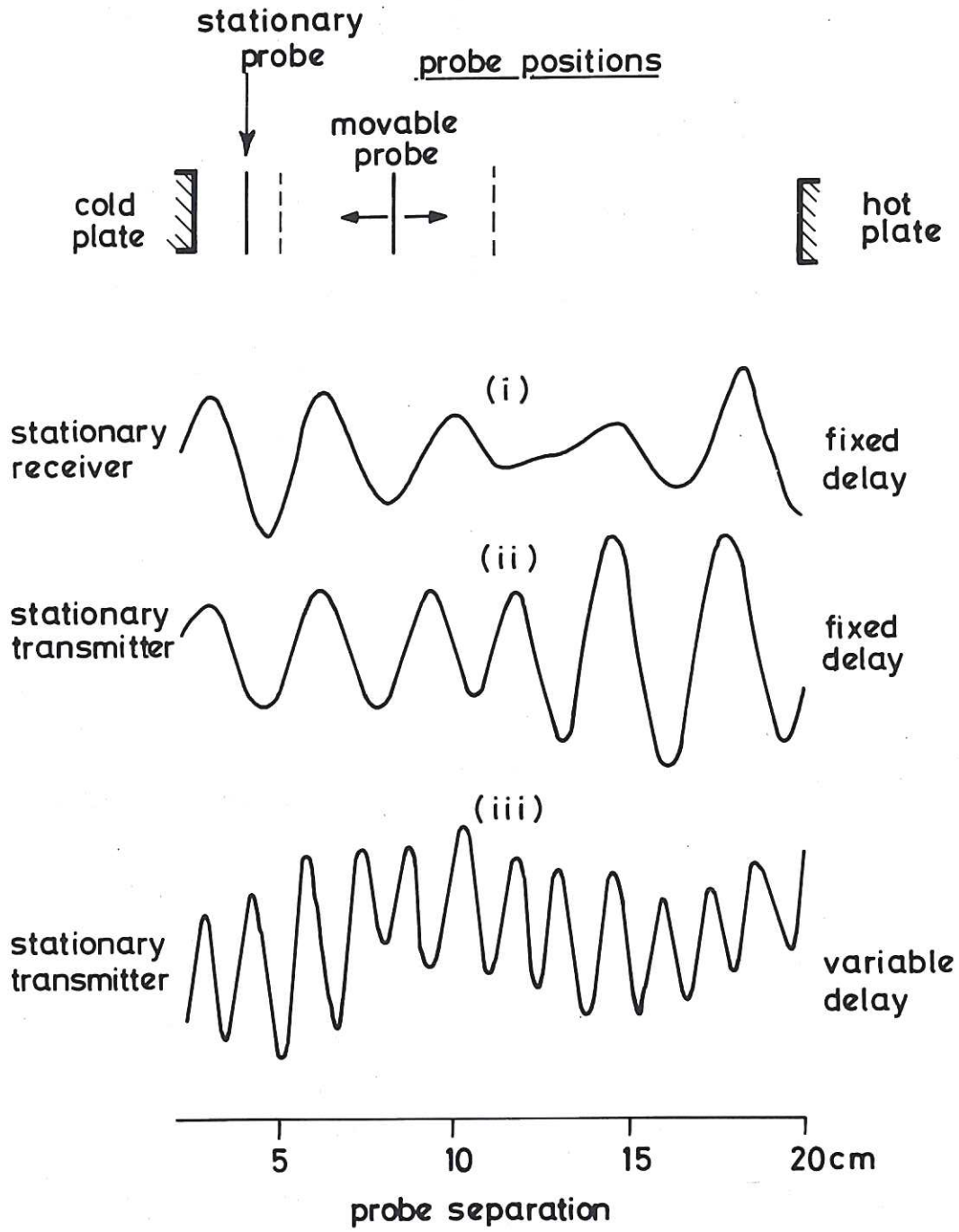

Fig.4 An example of interferometer traces at t = 0.3 μs for a transmitter frequency $\omega/2\pi$ = 320 MHz, plasma frequency $\omega_{pe}/2\pi$ = 540 MHz.
(i) & (ii) Traces obtained for parallel and antiparallel propagation respectively with a fixed sampling gate time-delay.
(iii) Trace obtained with a time-delay which increases at a rate of 0.001 μs per cm of probe separation; the antiparallel wavelength (calculated from (9) in the text) is 2.8 cm.

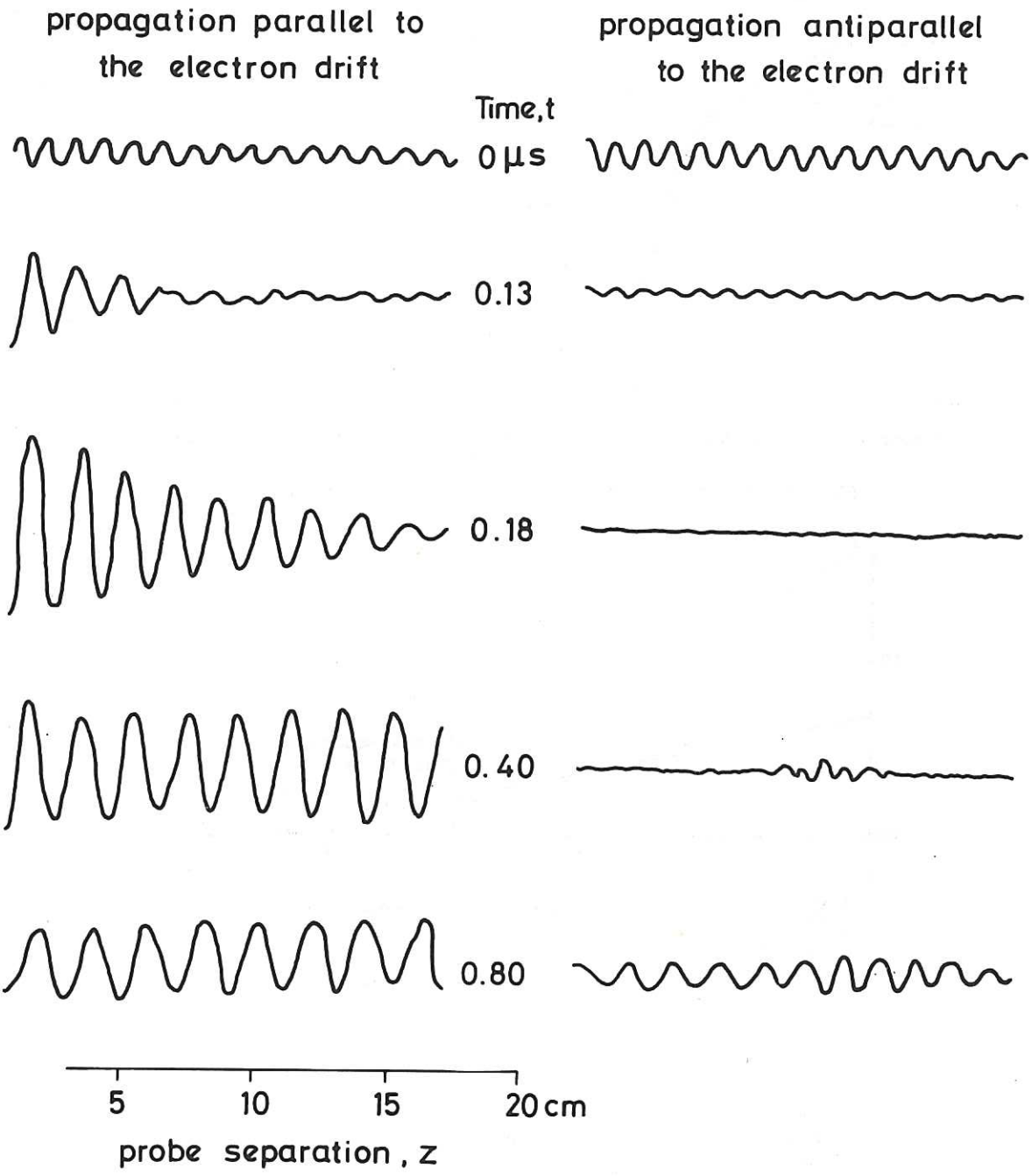

Fig.5 Typical interferometer traces at different times for $\omega/2\pi$ = 720 MHz, $\omega_{pe}/2\pi$ = 740 MHz.

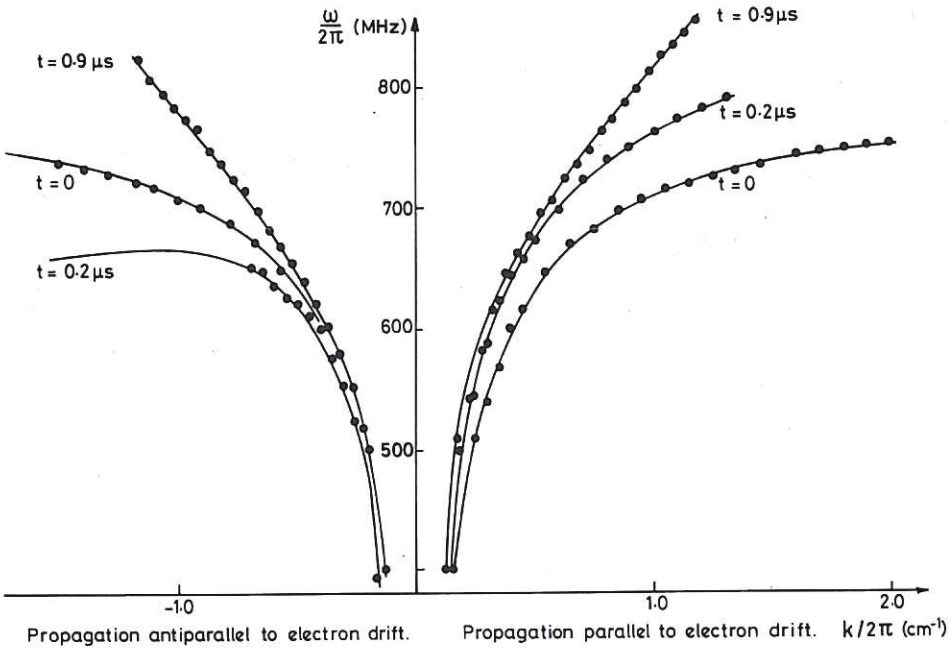

Fig.6 Typical set of dispersion curves measured at different times.

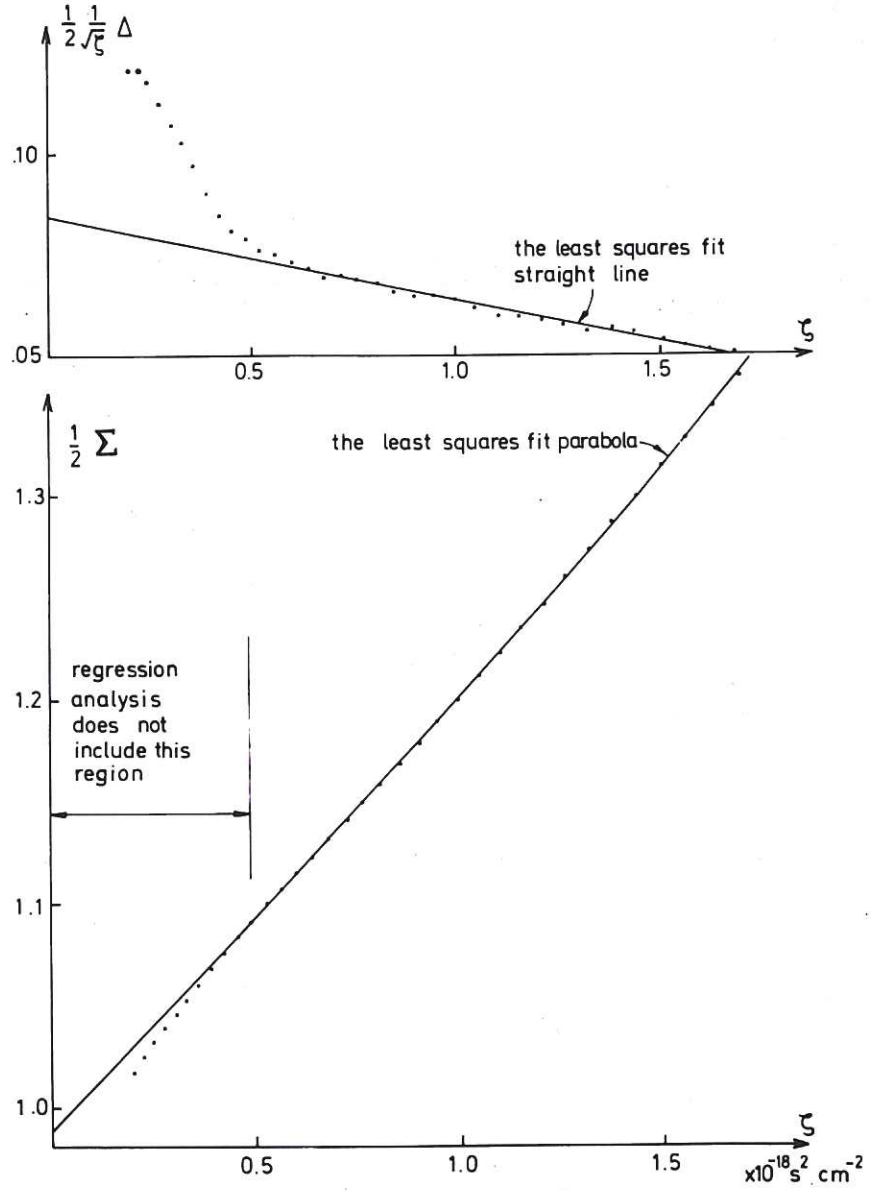

Fig.7 Typical plot of $\frac{1}{2}\Sigma$ and $\frac{1}{2}\frac{1}{\sqrt{\zeta}}\Delta$ versus ζ.

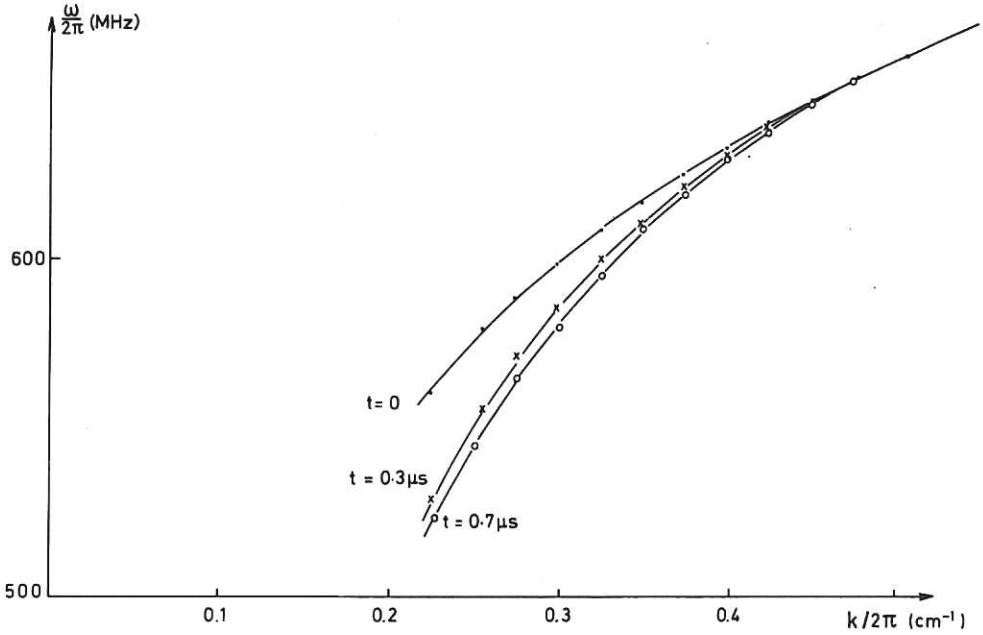

Fig.8 The change in the long wavelength dispersion (as viewed from the electron drift frame) when a large pulsed current of 700mA is drawn through the plasma column; $n_0 = 6 \times 10^9$ cm^{-3}.

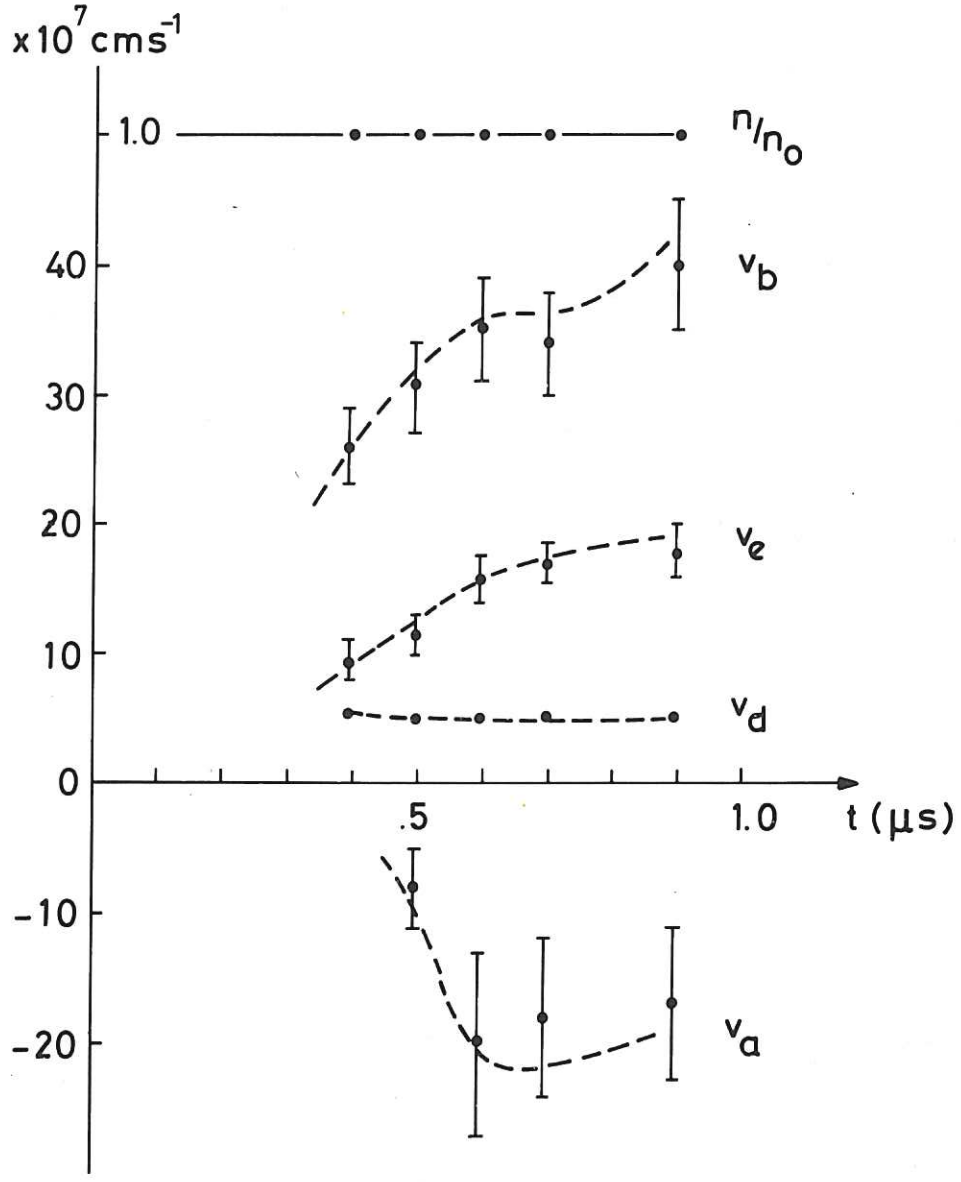

CLM-P 532

Fig.9 Evolution of the first five velocity moments (see text).